Video Article

Enhanced Electron Injection and Exciton Confinement for Pure Blue Quantum-Dot Light-Emitting Diodes by Introducing Partially Oxidized Aluminum Cathode

Zhibin Wang[1], Tai Cheng[1], Fuzhi Wang[1], Yiming Bai[1], Xingming Bian[1], Bing Zhang[1], Tasawar Hayat[2,3], Ahmed Alsaedi[3], Zhan'ao Tan[1]

[1]State Key Laboratory of Alternate Electrical Power System with Renewable Energy Sources, North China Electric Power University

[2]Department of Mathematics, Quaid-I-Azam University

[3]NAAM Research Group, Faculty of Science, King Abdulaziz University

Correspondence to: Zhan'ao Tan at tanzhanao@ncepu.edu.cn

URL: https://www.jove.com/video/57260
DOI: doi:10.3791/57260

Keywords: Retraction, Issue 135, Quantum Dots, Light-Emitting Diodes, LED, Autoxidation, Electron Injection, Luminance

Date Published: 5/31/2018

Citation: Wang, Z., Cheng, T., Wang, F., Bai, Y., Bian, X., Zhang, B., Hayat, T., Alsaedi, A., Tan, Z. Enhanced Electron Injection and Exciton Confinement for Pure Blue Quantum-Dot Light-Emitting Diodes by Introducing Partially Oxidized Aluminum Cathode. *J. Vis. Exp.* (135), e57260, doi:10.3791/57260 (2018).

Abstract

Stable and efficient red (R), green (G), and blue (B) light sources based on solution-processed quantum dots (QDs) play important roles in next-generation displays and solid-state lighting technologies. The brightness and efficiency of blue QDs-based light-emitting diodes (LEDs) remain inferior to their red and green counterparts, due to the inherently unfavorable energy levels of different colors of light. To solve these problems, a device structure should be designed to balance the injection holes and electrons into the emissive QD layer. Herein, through a simple autoxidation strategy, pure blue QD-LEDs which are highly bright and efficient are demonstrated, with a structure of ITO/PEDOT:PSS/Poly-TPD/QDs/Al:Al_2O_3. The autoxidized Al:Al_2O_3 cathode can effectively balance the injected charges and enhance radiative recombination without introducing an additional electron transport layer (ETL). As a result, high color-saturated blue QD-LEDs are achieved with a maximum luminance over 13,000 cd m^{-2}, and a maximum current efficiency of 1.15 cd A^{-1}. The easily controlled autoxidation procedure paves the way for achieving high-performance blue QD-LEDs.

Video Link

The video component of this article can be found at https://www.jove.com/video/57260/

Introduction

Light-emitting diodes (LEDs) based on colloidal semiconductor quantum dots have attracted great interest due to their unique advantages, including solution processability, tunable emission wavelength, excellent color purity, flexible fabrication, and low processing cost[1,2,3,4]. Since the first demonstrations of QDs-based LEDs in 1994, tremendous efforts have been devoted to engineering the materials and device structures[5,6,7]. A typical QD-LED device is designed to have a three-layered sandwich architecture which consists of a hole transport layer (HTL), an emissive layer, and an electron transport layer (ETL). The choice of a suitable charge transport layer is critical to balance the injected holes and electrons into the emissive layer for radiative recombination. Currently, vacuum-deposited small molecules are widely used as ETL, for instance, bathocuproine (BCP), tris(8-Hydroxyquinolinate) (Alq_3), and 3-(biphenyl-4-yl)-5-(4-tertbutylphenyl)-4-phenyl-4H-1,2,4-triazole (TAZ)[8]. However, the unbalanced carrier injection often causes the recombination region shift to ETL, making unwanted parasitic electroluminescence (EL) emission and deteriorating the device performance[9].

To enhance the device efficiency and environmental stability, solution-processed ZnO nanoparticles were introduced as an electron transport layer instead of the vacuum-deposited small-molecule materials. Highly bright RGB QD-LEDs were demonstrated for conventional device architecture, showing luminance up to 31,000, 68,000, and 4,200 cd m^{-2} for emission of orange-red, green, and blue, respectively[10]. For an inverted device architecture, high performance RGB QD-LEDs with low turn on voltage were successfully demonstrated with brightness and external quantum efficiencies (EQE) of 23,040 cd m^{-2} and 7.3% for red, 218,800 cd m^{-2} and 5.8% for green, and 2,250 cd m^{-2} and 1.7% for blue, respectively[11]. To balance the injected charges and preserve the QDs emissive layer, an insulating poly(methylmethacrylate) (PMMA) thin film was inserted between the QDs and ZnO ETL. The optimized deep-red QD-LEDs exhibited high external quantum efficiencies up to 20.5% and a low turn-on voltage of only 1.7 V[12].

Besides, optimizing the optoelectronic properties and nanostructures of QDs also plays a crucial role in boosting the device performance. For instance, highly fluorescent blue QDs with photoluminescence quantum yield (PLQE) up to 98% were synthesized through optimizing the ZnS shelling time[13]. Similarly, high-quality, violet-blue QDs with near 100% PLQE were synthesized by precisely controlling the reaction temperature. The violet-blue QDs-LED devices showed remarkable luminance and EQE up to 4,200 cd m^{-2} and 3.8%, respectively[14]. This synthesis method is also applicable to violet ZnSe/ZnS core/shell QDs, the QD-LEDs exhibited high luminance (2,632 cd m^{-2}) and efficiency (EQE=7.83%) by using Cd-free QDs[15]. Since blue quantum dots with high PLQE have been demonstrated, high charge injection efficiency in the QDs layer plays

another crucial role in fabricating high performance QD-LEDs. By substituting long chain oleic acid ligands to shorten 1-octanethiol ligands, the electron mobility of QDs film was increased two-fold, and a high EQE value over 10% was obtained[16]. The surface ligand exchange can also improve the morphology of QDs film and suppress the photoluminescence quenching among QDs. For instance, QDs-LED showed improved device performance by using chemically grafted QDs-semiconducting polymer hybrids[17]. Besides, high-performance QDs were prepared through reasonable optimization of the graded composition and thickness of the QDs shell, due to the enhanced charge injection, transport, and recombination[18].

In this work, we introduced a partial autoxidized aluminum (Al) cathode to improve the performance of ZnCdS/ZnS graded core/shell-based blue QD-LEDs[19]. The change of the potential energy barrier of the Al cathode was confirmed by ultraviolet photoelectron spectroscopy (UPS) and X-ray photoelectron spectroscopy (XPS). Furthermore, the fast charge carrier dynamics at the QDs/Al and QDs/Al:Al_2O_3 interface were analyzed by time-resolved photoluminescence (TRPL) measurements. In order to further validate the influence of partially oxidized Al on device performance, QD-LEDs with different cathodes (Al only, Al:Al_2O_3, Al_2O_3/Al, Al_2O_3/Al:Al_2O_3, and Alq_3/Al) were fabricated. As a result, high performance pure blue QD-LEDs were demonstrated by employing Al:Al_2O_3 cathodes, with a maximum luminance of 13,002 cd m^{-2} and a peak current efficiency of 1.15 cd A^{-1}. Furthermore, there was no additional organic ETL involved in the device architecture, which can avoid unwanted parasitic EL to guarantee the color purity under different working voltages.

Protocol

1. Pattern Etching of Indium Tin Oxide (ITO) Glass

1. Cut large pieces of ITO glass (12 cm × 12 cm) into 15 mm wide strips. Clean the ITO glass surface using a dust-free cloth with alcohol.
2. Check the conductive side of the ITO glass with a digital multimeter. Cover the active area of the ITO glass with adhesive tape, so that the active area is 2 mm wide in the middle.
3. Pour the zinc powder on the ITO glass (to a thickness of about 0.5 mm).
4. Pour the hydrochloric acid solution (36 wt%) onto the surface of the ITO glass and allow the ITO glass to completely soak in hydrochloric acid solution, then etch for 15 s.
5. Pour out the hydrochloric acid solution after corrosion, then rinse the ITO glass with water immediately. Remove the adhesive tape on the ITO glass.

2. Cleaning the ITO Glass

1. Immerse the ITO glass in a petri dish containing acetone solution for 15 min. Wipe off the glue on the ITO glass using a cotton ball.
2. Cut the ITO glass into square pieces (approximately 15 mm × 15 mm) with a glass cutter.
3. Sonicate the ITO glass sequentially in detergent water, tap water, deionized water, acetone, and isopropyl alcohol for 15 min.
4. Blow-dry the ITO glass with nitrogen gas followed by drying in an oven at 150 °C for 5 min in air atmosphere.
5. Put the cleaned ITO glass into an ultraviolet-ozone chamber and treat for 15 min.

3. Fabrication of a Hole Injection Layer

1. Take out the poly(3,4-ethylenedioxythiophene):poly(styrene sulfonate) (PEDOT:PSS) solution from the refrigerator. Stir the PEDOT:PSS solution at room temperature for 20 min to obtain an evenly dispersed solution.
   NOTE: The UV-Ozone treatment (Section 2.5) and agitation of PEDOT:PSS solution should be carried out simultaneously to avoid UV-Ozone treatment failure. Room temperature is maintained at 25 °C.
2. Take about 2 mL of PEDOT:PSS solution with a 10 mL syringe, and install a 0.45 µm polyether sulfone (PES) filter on the syringe.
3. Place the ITO glass at the center of the spin-coater. Pour two drops of the PEDOT:PSS solution onto the ITO glass.
4. Spin-coat the filtered PEDOT:PSS solution on the ITO substrate at 3,000 rpm for 30 s and then anneal the PEDOT:PSS-coated ITO at 150 °C for 15 min to give a 30 nm PEDOT:PSS film.

4. Fabrication of a Hole Transport Layer

NOTE: The hole transport layer and the emissive layer are fabricated in a nitrogen-filled glove-box with controlled oxygen and water concentration below 50 ppm.

1. Dissolve poly(N,N′-bis(4-butylphenyl)-N,N′-bis(phenyl)-benzidine) (Poly-TPD) in o-dichlorobenzene (1 mL) with a concentration of 25 mg mL^{-1}. Stir at room temperature overnight in the nitrogen-filled glove-box.
2. Pour 35 µL of Poly-TPD solution onto the PEDOT:PSS-coated ITO. Spin-coat the Poly-TPD solution at 3,000 rpm for 30 s to give a 40 nm Poly-TPD film, and then anneal at 150 °C for 30 min.

5. Fabrication of an Emissive Layer

1. Dissolve ZnCdS/ZnS quantum dots in toluene solution (300 µL) with a concentration of 14.3 mg mL^{-1}.
2. Pour 35 µL of the ZnCdS/ZnS solution onto the top of the Poly-TPD. Spin-coat the ZnCdS/ZnS solution at 3,000 rpm for 30 s to give a 40 nm film.
   NOTE: Baking is not necessary.

6. Vacuum Deposition

1. After a pressure of 10^{-4} Pa is reached, deposit the aluminum Tris(8-Hydroxyquinolinate) (Alq_3) on the substrates with a rate of 0.3 Å s^{-1} in a thermal evaporation chamber to give a 15 nm Alq_3 film.
   NOTE: The Alq_3 is deposited only for the device structure of ITO/PEDOT:PSS/Poly-TPD/QDs/Alq_3/Al.
2. Scrape a 2 mm wide active layer with a scraper to expose the ITO glass substrate.
3. Place the substrates in a metal mask and transfer them into a thermal evaporation chamber. Deposit the aluminum electrode with a rate of 1 Å s^{-1} to give a 100 nm Al film.

7. Autoxidation Procedure

1. Transfer the as-prepared Al cathode into a vacuum oven, and then pump air out of the oven until it is almost a vacuum.
2. Open the deflation valve and inject anhydrous compound air (O_2=20%, N_2=80%) into the vacuum oven with a pressure of 3×10^4 Pa. Oxidize for 0, 4.5, 12, and 17 h at room temperature (in the oven).

Representative Results

UV-Vis absorption and photoluminescence (PL) spectra were used to record the optical properties of ZnCdS/ZnS graded core/shell-based blue QDs. Transmission electron microscopy (TEM) and scanning electron microscopy (SEM) images were collected for the morphologies of QDs (**Figure 1**). X-ray photoelectron spectroscopy (XPS), electrochemical study, and ultraviolet photoelectron spectroscopy (UPS) were employed to detect the structural properties and energy levels of QDs (**Figure 2**). Time-resolved photoluminescence (TRPL) measurements were used to detect the fast charge carrier dynamics at the interface between QDs/Al and QDs/Al:Al_2O_3 (**Figure 3**). Finally, EL performance of QD-LEDs was performed (**Figure 4**, **Figure 5**, and **Table 1**).

Figure 1a shows the UV-vis absorption and PL emission spectra of the ZnCdS/ZnS graded core/shell-based blue QDs dispersed in toluene. The QDs solution showed an absorption edge at ~456 nm and a pure deep-blue emission peak located at 451 nm with a narrow full width at half maximum (FWHM) of only 17.8 nm. Sketch diagram of QDs in the inset show that the graded core/shell structure of QDs are capped with short-chain 1-octanethiol as surface ligands. By using a short-chain, 1-octanethiol molecule to replace long-chain organic molecules, the distance between QDs is shortened, which improves the charge injection properties in the QDs film. A representative transmission electron microscope (TEM) image of ZnCdS/ZnS blue QDs showed a relatively uniform size distribution, and the average diameter can be determined to be 14 ± 1.7 nm (**Figure 1b**). A continuous chemical composition gradient inside the QDs can be observed from the high resolution transmission electron microscope (HRTEM) image of a single ZnCdS/ZnS QD as shown in **Figure 1c**. **Figure 1d** shows the SEM image of the QDs layer spin-coated on the Poly-TPD substrate as used in device fabrication. A uniform and fully-covered QDs layer can be seen from the SEM image, which indicates the good film-forming properties of QDs.

The surface chemical characteristics of the autoxidized Al cathode were analyzed by XPS measurement. As shown in **Figure 2a**, the XPS spectrum of the Al 2p orbital can be fitted with three peaks. The peaks at 72.7, 74.3, and 75.5 eV correspond to metallic Al atoms, γ phase of Al_2O_3, and amorphous AlO_x[20]. Electrochemical cyclic voltammetry (CV) measurement has been performed to determine the valence band (VB) and conduction band (CB) energy levels of the ZnCdS/ZnS QDs[21]. As illustrated in **Figure 2b**, the onset oxidation potential and the onset reduction potential were determined to be -1.13 and 1.69 V, respectively. As a result, the VB and CB values for ZnCdS/ZnS QDs were calculated to be 3.58 and 6.4 eV, respectively. We measured the work functions of the QDs layer and the partially oxidized Al cathode by UPS (**Figure 2c**). The work functions of QDs and Al:Al_2O_3 were 3.87 and 3.5 eV, respectively, which were calculated by subtracting the energies at the secondary electron edges from the energy of the ultraviolet source He I (21.22 eV). The energy level diagram of the device is given in **Figure 2d**. **Figure 2e** and **Figure 2f** display the energy level alignment diagrams of the QDs layer with Al and Al:Al_2O_3. The work function and Fermi level of the Al cathode were taken from the previous report[22,23].

Next, we measured the TRPL spectra of the different QDs layers to determine the charge carrier dynamics (**Figure 3**). The TRPL curves were fitted by bi-exponential decays. For the QDs, QDs/Al and QDs/Al:Al_2O_3 samples, the average lifetimes were 8.945, 4.839, and 5.414 ns, respectively. Compared with the QDs/Al sample, the QDs/Al:Al_2O_3 sample exhibited a longer lifetime, which can be ascribed to the improvement of electron injection and the suppression of non-radiative recombination.

To further verify the effect of partially autoxidized Al cathode on the QD-LEDs device performance, QDs emissive layers contacted with different cathodes were fabricated. The performance parameters of QD-LEDs with different cathodes are summarized in **Table 1**. The device with pure Al cathode shows low brightness of 435 cd m^{-2} due to the inefficient charge injection (**Figure 4a**). In order to improve the electronic transmission ability, a 15 nm Alq_3 layer was introduced as ETL to balance the injected charges. As a result, the brightness of the QDs-LED device improved to 1,300 cd m^{-2}. After oxidation treatment, the QD-LEDs device (Al:Al_2O_3) exhibited a dramatically enhanced performance with a maximum luminance of 13,002 cd m^{-2} and a maximum current efficiency of 1.15 cd A^{-1}. Further insight into the relationship between device performance and oxidation treatment was gained by inserting an ultrathin Al_2O_3 layer (1.5 nm) as described in [24]. However, the Al_2O_3/Al device exhibited a maximum luminance of 352 cd m^{-2}, which has no enhancement compared with the bare Al-based device. The Al_2O_3/Al:Al_2O_3 device exhibited a modest level of luminance and efficiency (10,600 cd m^{-2} and 1.12 cd A^{-1}), and a relatively high turn-on voltage (defined as 1 cd m^{-2}) of 4.8 V. The CE-J curves of the QD-LEDs are shown in **Figure 4b**. The maximum efficiencies of the devices with Al:Al_2O_3 and Al_2O_3/Al:Al_2O_3 reached 1.15 and 1.12 cd A^{-1}, respectively, which was much higher than that of devices with Al, Al_2O_3/Al, and Alq_3/Al cathodes. In general, a high applied voltage will induce the spatial separation of electron and hole wave functions and should dramatically reduce the radiative recombination rate inside the QDs layer. The autoxidized Al:Al_2O_3 cathode can suppress exciton quenching at high current density, due to the enhanced electron injection and hole blocking abilities. **Figure 4c** depicts the J-V and L-V curves of QD-LEDs as a function of autoxidation time. The optimized device was achieved by using a 12 h autoxidized Al cathode.

Figure 5a shows the normalized EL spectra of QD-LEDs based on various cathodes. The EL peak of the Al:Al_2O_3 device was located at 457.3 nm with a FWHM of only 21.4 nm, which indicated a pure blue light without any parasitic EL emission. Contrastively, the EL spectrum based on Alq_3/Al cathode shows a parasitic EL originated from Alq_3. Stable EL emission can be observed from Al:Al_2O_3 based device under different applied biases (**Figure 5b**). As illustrated in **Figure 5c**, the coordinate of EL spectrum locates at very edge of the Commission Internationale de L'Eclairage (CIE) chromaticity diagram, resulting a high saturated color. **Figure 5d** shows the operating photographs of QD-LEDs, which can be easily prepared with large area of 1 cm^2.

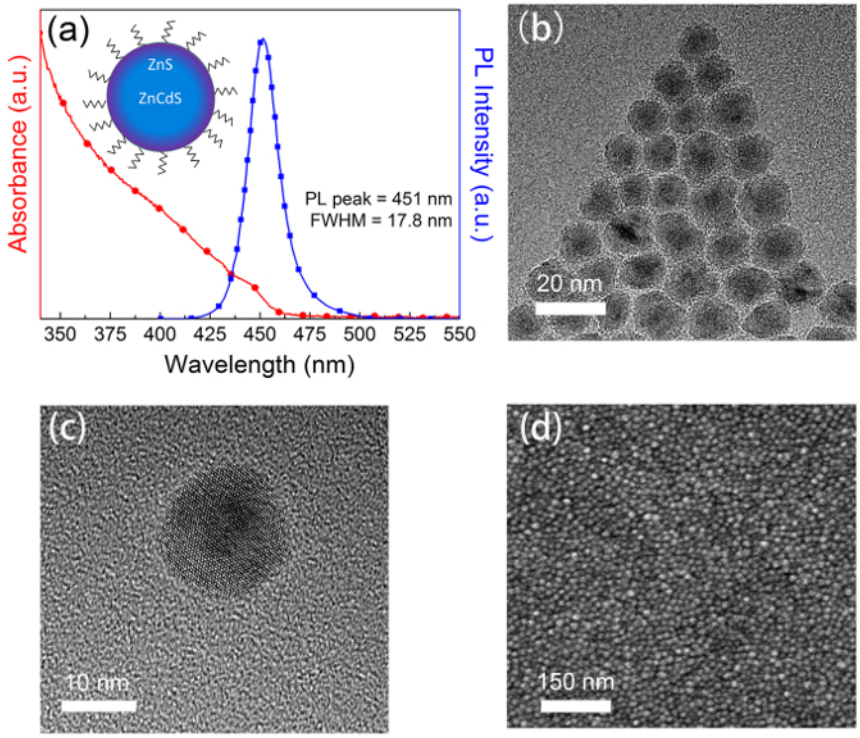

Figure 1: Optical properties and morphologies of ZnCdS/ZnS graded core/shell-based blue QDs. (**a**) Absorption and PL spectra of ZnCdS/ZnS QDs distributed in toluene solution. (**b**) TEM image and (**c**) HRTEM image of QDs. (**d**) SEM image of QDs film spin-coated on the Poly-TPD substrate as used in device fabrication. Reprinted with permission from [19]. Please click here to view a larger version of this figure.

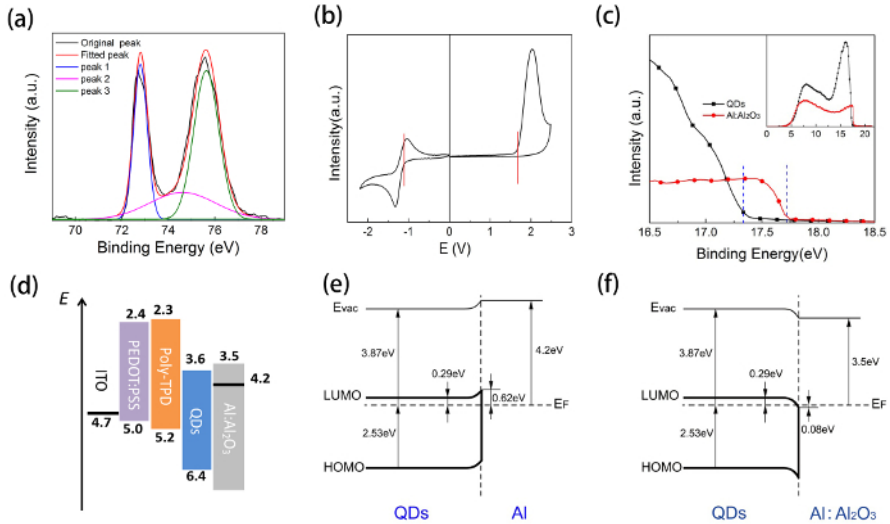

Figure 2: Use of X-ray photoelectron spectroscopy (XPS), electrochemical study, and ultraviolet photoelectron spectroscopy (UPS) to detect the structural properties and energy levels of QDs. (**a**) Al 2p orbital XPS spectra of autoxidized Al:Al_2O_3 cathode. (**b**) The cyclic voltammetry (CV) curves of the ZnCdS/ZnS QDs solution. (**c**) UPS spectra of the ZnCdS/ZnS QDs film and the autoxidized Al:Al_2O_3 cathode prepared on ITO substrates. Inset is the complete view of the spectra. (**d**) Flat band energy level diagram of the QD-LED device. (**e**) Energy level diagram at the QDs/Al interface and (**f**) the QDs/Al:Al_2O_3 interface. Reprinted with permission from [19]. Please click here to view a larger version of this figure.

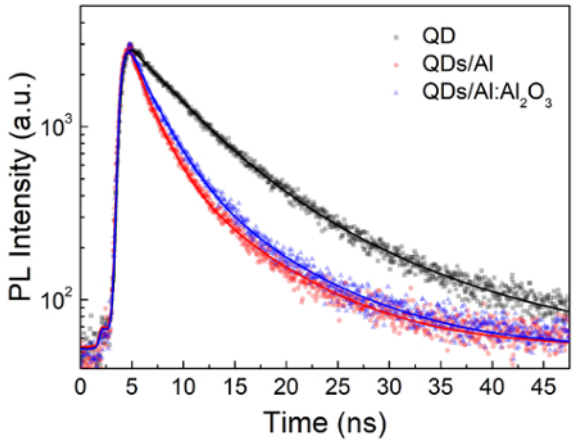

Figure 3: Time-resolved photoluminescence decay for the QDs films contacting with different layers. Reprinted with permission from reference[19]. The TRPL curves were fitted by bi-exponential decays. Compared with the QDs/Al sample, the QDs/Al:Al2O3 sample exhibits a longer lifetime, which can be ascribed to the improvement of electron injection and suppression of non-radiative recombination. Please click here to view a larger version of this figure.

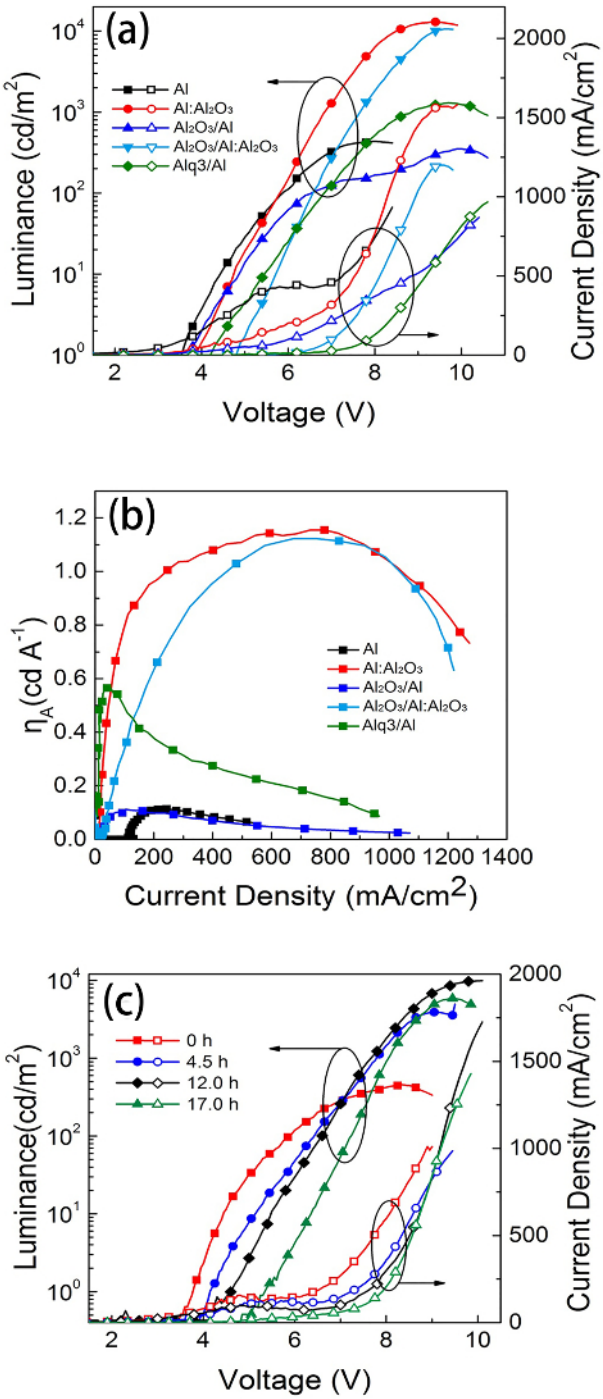

Figure 4: EL performance of QD-LEDs based on different cathodes. (**a**) Current density-luminance-voltage (J-L-V) and (**b**) current efficiency-current density (CE-J) characteristic curves of devices with different cathodes. (**c**) The J-L-V curves of devices with different Al cathodes autoxidized time. Reprinted with permission from[19]. Please click here to view a larger version of this figure.

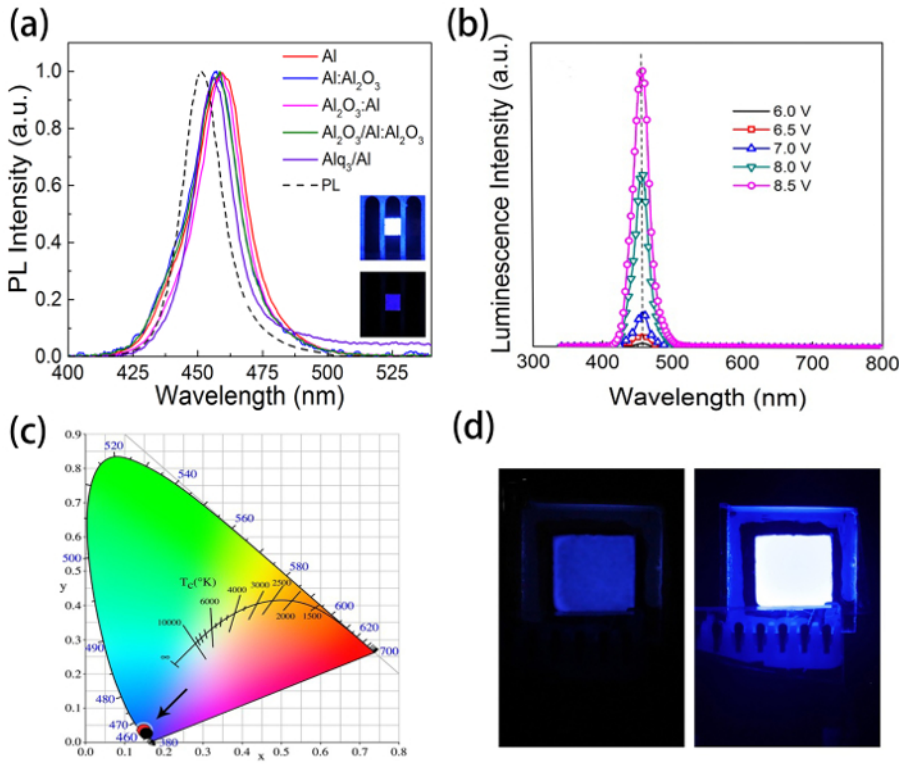

Figure 5: EL spectra, CIE coordinates and operating photographs of an Al:Al_2O_3 based QD-LEDs. (**a**) EL spectra of QD-LEDs based on Al, Al:Al_2O_3, Al_2O_3:Al, Al_2O_3/Al:Al_2O_3 and Alq_3/Al cathodes. Inset is the operating photographs of QD-LEDs with active area of 4 mm^2. (**b**) EL spectra of QD-LEDs derived from various biases. (**c**) CIE coordinates of the Al:Al_2O_3 based QD-LEDs. (**d**) Operating photographs of QD-LEDs with active area of 1 cm^2. Reprinted with permission from [19]. Please click here to view a larger version of this figure.

Type of Sample	Peak luminance	Peak current efficiency	Turn-on voltage	Emission peak	FWHM
	(cd m^{-2})	(cd A^{-1})	(V)	(nm)	(nm)
Al	435	0.11	3.56	459.1	22.5
Al:Al_2O_3	13002	1.15	3.83	457.3	21.4
Al_2O_3/Al	352	0.11	3.70	458.8	20.9
Al_2O_3/Al:Al_2O_3	10600	1.12	4.80	457.1	20.8
Alq_3/Al	1300	0.57	4.20	455.9	17.5

Table 1: EL parameters of QD-LEDs based on different cathodes. Reprinted with permission from reference[19].

Discussion

The device architecture of the blue QD-LED consists of an ITO transparent anode, a PEDOT:PSS HIL (30 nm), a Poly-TPD HTL (40 nm), a ZnCdS/ZnS QDs EML (40 nm), and an Al:Al_2O_3 cathode (100 nm). Due to the porous character of the Al cathode, we obtained an oxidized Al cathode by exposing it to oxygen. **Figure 2e** and **Figure 2f** display the energy level alignment diagrams of QDs layer with Al and Al:Al_2O_3. When the QDs contact with the Al cathode, a Schottky contact is formed at the QDs/Al interface, which introduces large internal resistance to hinder the electron injection from the cathode (**Figure 2e**). When the QDs contact the Al:Al_2O_3 cathode, an ohmic contact is formed at the QDs/Al:Al_2O_3 interface (**Figure 2f**), which reduces the electron injection barrier and accelerates the electron injection. The decrease of the potential energy barrier at QDs/cathode interface improved the electron injection efficiency and reduced the energy consumption. To further investigate the exciton quenching effect at the QDs/cathode interface, the TRPL spectra were analyzed (**Figure 3**). The QDs/Al:Al_2O_3 sample showed a longer PL decay time (5.414 ns) compared to that of the QDs/Al sample (4.839 ns), indicating alleviation of the luminescence quenching at QD/cathode interface[25,26]. Therefore, the enhanced device performance can be ascribed to the reduced potential barrier and the suppression of luminescence quenching.

The Al:Al_2O_3 cathode can be prepared by easily controlled autoxidation procedures. It should be Noted that there is no additional ETL involved in the protocol. The device performance is expected to be further improved after combining the autoxidized Al:Al_2O_3 cathode with other ETL (*e.g.*, ZnO)[12,13,15].

In conclusion, we have presented a novel method to improve both the brightness and efficiency of blue QD-LEDs using autoxidized Al cathode. High color-saturated blue QD-LEDs have been demonstrated with a peak luminance of 13,002 cd m^{-2} and a peak current efficiency of 1.15 cd A^{-1}, which is among the best performance reported in other works. The enhanced device performance can be ascribed to the improved electron injection and suppressed luminescence quenching. Therefore, the method presented in this protocol is an important step towards the realization of high-performance blue QD-LED devices.

Disclosures

We have nothing to disclose.

Acknowledgements

This work was supported by the NSFC (51573042), The National Key Basic Research Program of China (973 project, 2015CB932201), Fundamental Research Funds for the Central Universities, China (JB2015RCJ02, 2016YQ06, 2016MS50, 2016XS47).

References

1. Shirasaki, Y., Supran, G. J., Bawendi, M. G., & Bulović, V. Emergence of colloidal quantum-dot light-emitting technologies. *Nat. Photonics.* **7** (1), 13-23 (2012).
2. Chen, O., Wei, H., Maurice, A., Bawendi, M., & Reiss, P. Pure colors from core-shell quantum dots. *MRS Bull.* **38** (09), 696-702 (2013).
3. Dai, X., Deng, Y., Peng, X., & Jin, Y. Quantum-Dot Light-Emitting Diodes for Large-Area Displays: Towards the Dawn of Commercialization. *Adv. Mater.* **29** (14) (2017).
4. Wang, L. *et al.* High-performance azure blue quantum dot light-emitting diodes via doping PVK in emitting layer. *Org. Electron.* **37,** 280-286 (2016).
5. Colvin, V., Schlamp, M., & Alivisatos, A. P. Light-emitting diodes made from cadmium selenide nanocrystals and a semiconducting polymer. *Nature.*, **370** (6488), 354-357 (1994).
6. Tan, Z. *et al.* Colloidal nanocrystal-based light-emitting diodes fabricated on plastic toward flexible quantum dot optoelectronics. *J. Appl. Phys.* **105** (03), 034312 (2009).
7. Tan, Z. *et al.* Bright and color-saturated emission from blue light-emitting diodes based on solution-processed colloidal nanocrystal quantum dots. *Nano Lett.* **7** (12), 3803-3807 (2007).
8. Lee, C.-L., Nam, S.-W., Kim, V., Kim, J.-J., & Kim, K.-B. Electroluminescence from monolayer of quantum dots formed by multiple dip-coating processes. *physica status solidi (b).* **246** 803-807 (2009).
9. Lee, T.-C. et al. Rational Design of Charge-Neutral, Near-Infrared-Emitting Osmium(II) Complexes and OLED Fabrication. *Advanced Functional Materials.* 19, 2639-2647 (2009).
10. Qian, L., Zheng, Y., Xue, J., & Holloway, P. H. Stable and efficient quantum-dot light-emitting diodes based on solution-processed multilayer structures. *Nat. Photonics.* **5** (9), 543-548 (2011).
11. Kwak, J. *et al.* Bright and efficient full-color colloidal quantum dot light-emitting diodes using an inverted device structure. *Nano Lett.* **12** (5), 2362-2366 (2012).
12. Dai, X. *et al.* Solution-processed, high-performance light-emitting diodes based on quantum dots. *Nature.* **515** (7525), 96-99 (2014).
13. Lee, K.-H., Lee, J.-H., Song, W.-S., Ko, H., Lee, C., Lee, J.-H., Yang, H. Highly efficient, color-pure, color-stable, blue quantum dots light-emitting devices. *ACS Nano.* **7** (8), 7295-7302 (2013).
14. Shen, H. *et al.* High-efficient deep-blue light-emitting diodes by using high quality ZnxCd1-xS/ZnS core/shell quantum dots. *Adv. Funct. Mater.* **24** (16), 2367-2373 (2014).
15. Wang, A. *et al.* Bright, efficient, and color-stable violet ZnSe-based quantum dot light-emitting diodes. *Nanoscale.* **7** (7), 2951-2959 (2015).
16. Shen, H. *et al.* High-efficiency, low turn-on voltage blue-violet quantum-dot-based light-emitting diodes. *Nano Lett.* **15** (2), 1211-1216 (2015).
17. Fokina, A. *et al.* The role of emission layer morphology on the enhanced performance of light-emitting diodes based on quantum dot-semiconducting polymer hybrids. *Adv. Mater. Interfaces.* **3** (18), 1600279 (2016).
18. Yang, Y. *et al.* High-efficiency light-emitting devices based on quantum dots with tailored nanostructures. *Nat. Photonics.* **9**, 259-266 (2015).
19. Cheng, T. *et al.* Pure Blue and Highly Luminescent Quantum-Dot Light-Emitting Diodes with Enhanced Electron Injection and Exciton Confinement via Partially Oxidized Aluminum Cathode. *Adv. Opt. Mater.* **5** (11), 1700035 (2017).
20. Rotole, J. A., & Sherwood, P. M. A. Gamma-Alumina (γ-Al2O3) by XPS. *Surf. Sci. Spectra.* **5** (1), 18-24 (1998).
21. Liu, J., Yang, W., Li, Y., Fan, L., & Li, Y. Electrochemical studies of the effects of the size, ligand and composition on the band structures of CdSe, CdTe and their alloy nanocrystals. *Phys. Chem. Chem. Phys.* **16** (10), 4778-4788 (2014).
22. Abbaszadeh, D., Wetzelaer, G. A. H., Doumon, N. Y., & Blom, P. W. M. Efficient polymer light-emitting diode with air-stable aluminum cathode. *J. Appl. Phys.* **119** (9), 095503 (2016).
23. Yu, L. *et al.* Optimization of the energy level alignment between the photoactive layer and the cathode contact utilizing solution-processed hafnium acetylacetonate as buffer layer for efficient polymer solar cells. *Acs Appl. Mater. Interfaces.*, **8** (1), 432-441 (2016).
24. Li, F., Tang, H., Anderegg, J., & Shinar, J. Fabrication and electroluminescence of double-layered organic light-emitting diodes with the Al2O3/Al cathode. *J. Shinar, Appl. Phys. Lett.* **70** (10), 1233-1235 (1997).
25. Bai, Z. et al. Hydroxyl-Terminated CuInS2Based Quantum Dots: Toward Efficient and Bright Light Emitting Diodes. *Chemistry of Materials.* 28, 1085-1091 (2016).
26. Wang, Z. et al. Efficient and Stable Pure Green All-Inorganic Perovskite CsPbBr3 Light-Emitting Diodes with a Solution-Processed NiOx Interlayer. *The Journal of Physical Chemistry C.* (2017).

